# SINGLE IONS IN PAUL TRAPS

F. SCHMIDT-KALER, CH. ROOS, H. C. NÄGERL, H. ROHDE, S. GULDE, A. MUNDT, TH. ZEIGER, G. REYMOND, G. THALHAMMER, D. LEIBFRIED, J. ESCHNER, AND R. BLATT

*Institut für Experimentalphysik, Universität Innsbruck, Technikerstraße 25, A-6020 Innsbruck, Austria, http:heart-c704.uibk.ac.at*

The use of trapped ions for quantum information processing requires the preparation of linear strings of ions at low temperatures and the coherent manipulation of the quantum state of an individual ion in the string by laser light. In our experiment, $^{40}Ca^+$ ions are trapped in a linear Paul trap, forming crystallized linear strings when laser cooled. These strings are observed by fluorescence detection on the $S_{1/2} - P_{1/2}$ dipole transition at 397nm using a photomultiplier and a CCD camera. The narrow $S_{1/2} - D_{5/2}$ quadrupole transition at 729nm can then be used to investigate and manipulate the vibrational motion of the ion in the trap. Experimentally, the spectral resolution obtained on this transition is 1kHz proving a long coherence time for the two-level system. Ions in a superposition of the $S_{1/2}$ and $D_{5/2}$ states are then suited as qubits and for quantum information processing. Single qubit rotations are realized by addressing individual ions in the string. This is achieved using a tightly focused laser beam at 729nm, which can be steered to the ions either using an acousto-optic deflector or by shifting the ions using additional fields. Individual addressing is detected by the observation of quantum jumps to the $D_{5/2}$ level. Eventually, the realization of a two-ion quantum gate requires ground state cooling of the string. We have applied sideband cooling to a single $Ca^+$ ion in a three-dimensional Paul trap and reached the ground state of vibration with 95% probability. This state provides the ideal initial conditions for coherent manipulation of internal and external degrees of freedom on the $S_{1/2} - D_{5/2}$ transition. Namely, if the laser detuning is chosen detuned from the bare transition frequency, Rabi oscillations of electronic excitation and vibrational state are expected. We have observed a large number ($\sim$30) of those oscillations for initial preparation in vibrational Fock states n=0 and n=1, thus showing a ms decoherence time. The status of current experiments, determining temperatures, cooling times and decoherence times for the single ion is reviewed and the application of experimental techniques for future experiments is discussed.

## 1 Introduction

One or a few ions stored in a radio-frequency Paul trap offer an ideal environment to study the dynamics of simple quantum systems. With the aid of laser pulses, the investigator can tailor the interactions and dynamics of this system almost at will. Quantum information processing, as well as the study of foundations of quantum mechanics, ultrahigh precision spectroscopy, the investigation of future frequency standards, and last but not least the investigation of decoherence, are possible applications of the perfect control of internal and external quantum mechanical degrees of freedom of a string of trapped ions [1,2,3,4]. A particulary interesting situation arises when a suitable laser light field couples the motion of the ion(s) in the trapping potential with their electronic levels. This situation is described by an interaction Hamiltonian acting on two internal electronic levels, $|s\rangle$ and $|d\rangle$, with energy difference $\nu_{sd}$, which are 'dressed' by the harmonic oscillator states $|n\rangle$ of the external motion at frequency $\nu_{trap}$.

The interaction Hamiltonian takes the form

$$H_{\text{int}} = -\hbar\Omega \left(\sigma^{+} e^{i\eta(a^{\dagger}+a)} + \sigma^{-} e^{-i\eta(a^{\dagger}+a)}\right), \tag{1}$$

where $\eta = k\sqrt{h/2m\nu_{trap}}$ is the Lamb-Dicke parameter, $(a^{\dagger}+a)$ the position operator in terms of creation and annihilation operators for the harmonic oscillator, and $\Omega$ is the coupling strength proportional to the amplitude of the laser light field. This interaction Hamiltonian is inherently richer than the classical Jaynes Cummings Hamiltonian [5,6], but reduces to the latter in the so-called Lamb-Dicke limit $\eta \cdot \sqrt{\langle(a^{\dagger}+a)^2\rangle} << 1$ and when the detuning of the light field with respect to $\nu_{sd}$ is $\delta = -\nu_{trap}$. We assume that the radiative width of both levels $|s\rangle$ and $|d\rangle$ is much smaller than $\nu_{trap}$, such that the motional sidebands of the atomic resonance, i.e. transitions such as $|s,n\rangle$ to $|d,n\pm 1\rangle$, are well resolved. In general, any detuning $\delta = (n'-n)\cdot\nu_{trap}$ $(n,n'$ integer numbers) will resonantly drive transitions between the states $|s,n\rangle$ and $|d,n'\rangle$, and thus lead to a different interaction Hamiltonian.

## 2 Ion trapping

The experimental techniques to realize the well controlled situation described by the Hamiltonian above have historically evolved from efforts to build frequency standards with trapped and cooled ions [7,8]. Dynamical trapping of charged particles in radiofrequency (rf) traps has first been proposed and experimentally verified by W. Paul in 1958. An rf electric field, generated by an appropriate electrode structure, creates a pseudo-potential confining a charged particle [10].

In a *linear* Paul trap, the quadrupole rf field varies only in the xy-plane, such as in a quadrupole mass spectrometer, and an additional electrical dc potential provides confinement along the z-axis. A major advantage compared to a three-dimensional Paul trap is that the micromotion, i.e. the forced vibration induced by the rf field, vanishes for all ions on the z-axis. Furthermore the oscillation frequency in that direction can be chosen freely and independently from the radial secular frequencies. In contrast, in three-dimensional Paul traps Coulomb repulsion between ions pushes them into the rf field where

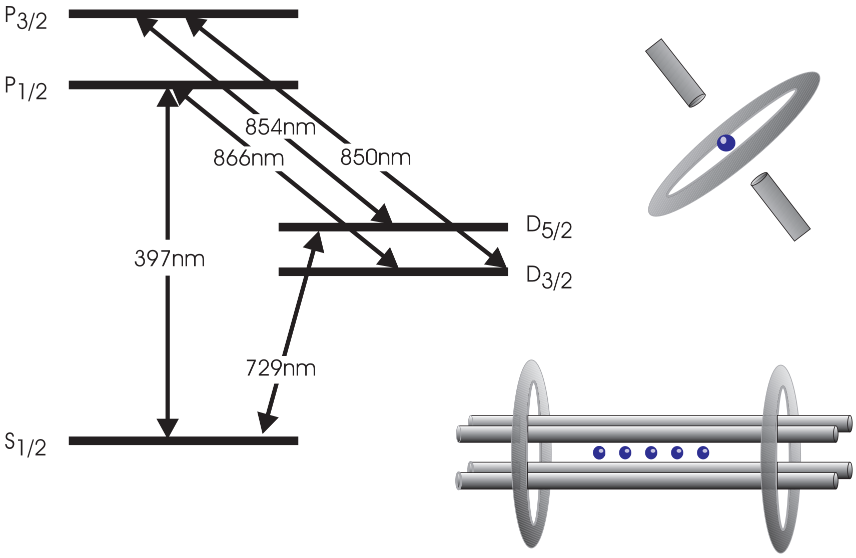


Figure 1. right: Schematic setup of the linear trap and the three-dimenional Paul trap. In the linear trap, confinement is maintained by the rf quadupole field in radial direction and by the dc potential of positively charged ring electrodes.
left: Level scheme of $^{40}Ca^{+}$. The lifetime of both D states is 1s. Superposition states of $|S_{1/2}\rangle$ and $|D_{5/2}\rangle$ are used to implement a qubit.

micromotion heating might occur. However, even if the use of linear traps for a larger number of ions seems favorable, an elongated version of the three-dimensional Paul trap has been used to produce strings of two and three ions [12].

Our *linear trap* [13] consists of 4 parallel steel rods with 2mm spacing, diagonally connected to generate the quadrupole rf field for radial confinement, see Fig.1. The rf field at $\Omega/2\pi = 15.9$MHz yields a radial trapping pseudo-potential with secular frequencies of $\nu_r \leq 2.5$MHz. Two DC ring electrodes of 4mm diameter and 10mm spacing serve as the axial endcaps for longitudinal confinement. DC voltages up to 2000V on the ring electrodes result in a harmonic trapping potential at an axial frequency of $\nu_z \leq 700$kHz. Our *three-dimensional trap* consists of a ring electrode (diameter 1.4mm) and two dc endcaps (distance 1.2mm), see Fig.1. An rf field at 20.3MHz with few hundred volts amplitude yields $\nu_{axial} \leq 2$MHz, $\nu_{radial} \leq 1$MHz. The relatively large dimensions of our traps help to reduce unwanted interactions between the ions and surface charges on the electrodes [14]. Ions are produced from an atomic beam by electron impact ionization inside the trap, where they are subsequently confined and laser cooled [15].

## 3 Laser Doppler cooling and ion detection

We have chosen $^{40}Ca^{+}$ ions for the experiments since their excitation wavelengths are relatively easy to generate with solid state and diode lasers. See Fig. 1 for the relevant atomic levels. Laser light at 397nm is generated with a frequency doubled Ti:Sapphire laser at 794nm while the light sources at 866nm, 854nm and 850nm are grating stabilized diode lasers. With Doppler cooling on the dipole-allowed transition at 397nm we reach a temperature near the Doppler cooling limit of 0.5mK. The fluorescence of the ions at 397nm is imaged through two optical viewports using f/1.3 collimation lenses onto a photomultiplier and an intensified CCD camera. To excite the $S_{1/2}$-$D_{5/2}$ transition at 729nm we use a Ti:Sapphire laser, that has been frequency stabilized to below 1kHz.

## 4 Individual addressing of ions in a string

With the imaging optics and the CCD camera, we can easyly resolve individual ions in a trapped string. Taking advantage of the 4$\mu$m optical resolution at 397nm, we use the same optical path also for individual addressing. The ingoing laser beam at 729nm is separated from the outgoing uv fluorescence with a dichroic mirror. An optical fiber between laser and trap setup provides stable alignment, and a telescope is used to adjust the $\lambda$=729nm beam parameters for optimum focusing. Between fiber exit and telescope, an acousto-optical modulator is used to shift the direction of the addressing beam.

We have experimentally demonstrated two ways of addressing with a string of 3 ions [16]: First, we used the tightly focused 729nm laser beam at a fixed position and shifted the ion string by slight variation of the endcap ring electrode voltages (less than 1%). Secondly, we fixed the ion string position and moved the laser beam over the string with an acousto-optical modulator (AOM). The optical excitation sequence consists of three parts: A 0.5ms excitation period with light at 729nm is followed by a detection period with the lasers at 397nm and 866nm on (2ms), during which we register for all three ions the probability $P_D$ that the transition to the metastable $D_{5/2}$ level has occured. The sequence is closed by a cooling and repumping period with the lasers at 397nm, 866nm and 854nm on (2ms) which prepares the ions in the $S_{1/2}$ state for the next 729nm pulse.

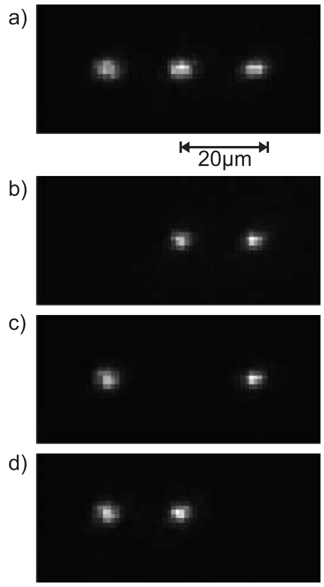


Figure 2. a): Fluorescence at 397nm of three ions imaged onto the CCD camera. The distance between ions is $19\mu$m ($\omega_z$ =125(0.2)kHz) and the spatial resolution for uv is near $4\mu$m. The exposure time is 1s.
b) - d): Different ions in the string are addressed with focused laser light at 729nm and transferred into the non-fluorescing $D_{5/2}$ state.

We obtain a resolution of spatial *addressing* of $w \leq 6\mu$m. In Fig. 2 (b) - (d) we show CCD images of the addressed string with different ions transferred to the non-fluorescing $D_{5/2}$ state. Having shown sufficiently good spatial resolution for individual addressing, we implemented the second scheme that is directly applicable to future quantum information processing. Shifting the ion string does not allow sufficiently fast switching for longer ion strings, since a fast, non-adiabatic shift of position causes heating [14]. Therefore, for fast addressing, the laser beam position is shifted by the AOM. From the experimental data, we obtained again a $6\mu$m addressing resolution [16].

## 5 Normal modes of oscillation

Small displacements of the ions from their equilibrium positions are described in terms of normal modes [20]. After loading the linear trap with a string of ions, we excited normal modes by applying additional ac-voltages to one of the ring electrodes [19]. The normal mode oscillation has been observed stroboscopically with the gated CCD camera by accumulating images at the same phase of the exciting electric field. We measured the excitation frequency of the center-of-mass mode and of the so called beathing mode where the oscillation amplitude of each ion is proportional to its distance from the center. The ratio of these

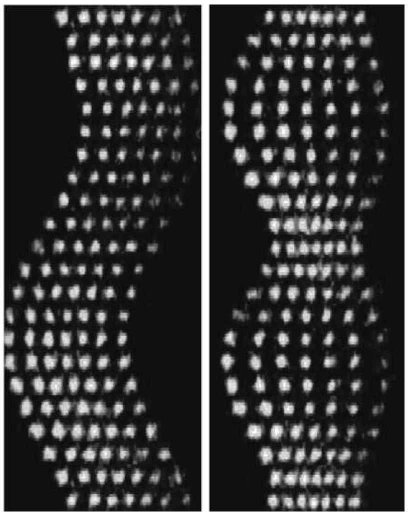

Figure 3. Stroboscopic image of the rf-excited center-of-mass motion at 158.5kHz (left) and breathing mode motion at 276.0kHz (right). Time increases from bottom to top by a fraction of the oscillation period per frame. For animated pictures see also our web-page.

frequencies agrees within 1% with the expected value of $\sqrt{3}$. Fig. 3 shows the excitation of the center-of-mass mode and the breathing mode.

## 6 Spectroscopy of the $S_{1/2} - D_{5/2}$ transition

We use laser pulses of fixed duration at 729nm that couple the $S_{1/2}$ and $D_{5/2}$ states. After preparing the $m_J = +1/2$ sub-state of $S_{1/2}$ by optical pumping, we excite the ion into one substate of the $D_{5/2}$ state manifold. A magnetic field is used to Zeeman-split the transitions to different $m_J$ levels in frequency. In the final step of this 'quantized spectroscopy', we detect whether a transition to the shelving level $D_{5/2}$ has been induced. The above sequence is repeated typically 100 times to measure the excitation probability $P_D$ for any set of parameters. In this way we study the dependance of $P_D$ on experimental parameters such as the detuning $\Delta\nu$ of the light at 729nm with respect to the ionic transition or the length of the excitation pulse. The duration of a single sequence is typically 5ms or less, and we can synchronize the sequence with the ac power line at 50Hz, which reduces ac-magnetic field fluctuations, although at the cost of slower data aquisition. A detailed description of the specific features of $S_{1/2} - D_{5/2}$ spectroscopy in our linear trap is given in [11]. In the following, we focus to the spectrum of excitation $P_D(\nu)$ for a *single ion in the three-dimensional* trap at the Doppler limit, see Fig. 4a, which shows a central 'carrier' peak with red and blue sideband at the trap frequencies $\nu_{axial}$

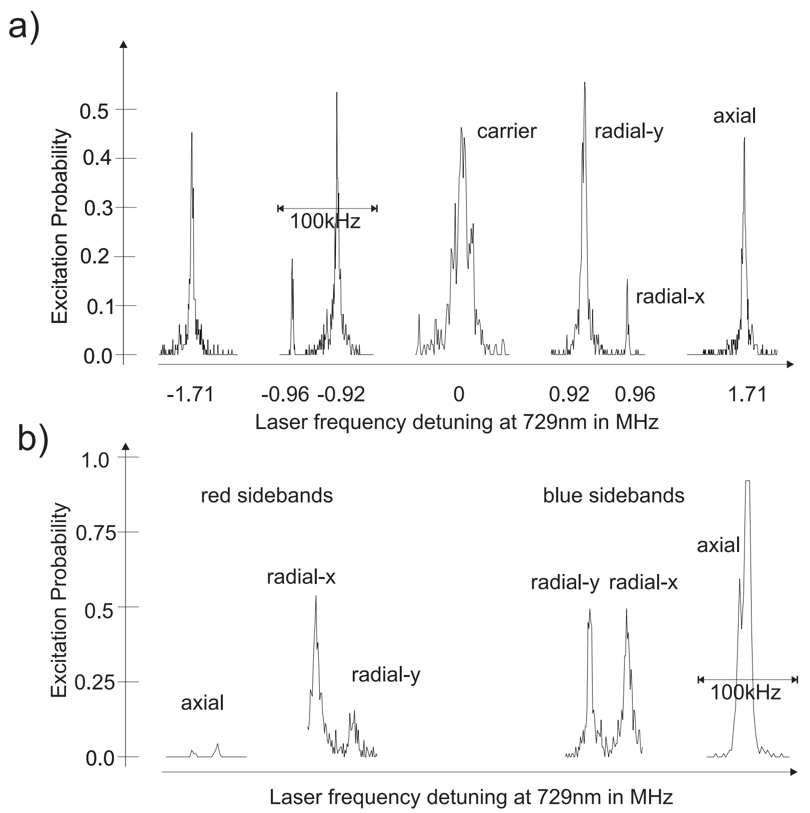


Figure 4. a) Sideband spectrum of the $S_{1/2}, m_J = 1/2 - D_{5/2}, m_J = 5/2$ transition obtained with a single ion in the three-dimensional trap. See the axial, radial-y, and radial-x sidebands at frequency detunings of $\pm$ 1.71MHz, $\pm$ 960kHz and $\pm$ 920kHz. The excitation of red and corresponding blue sideband is equal at the Doppler limit $\langle n_{ax.} \rangle \approx 7$ and $\langle n_{rad.} \rangle \approx 12$. The Lamb Dicke factor is calculated with $\eta_{ax.}$ and $\eta_{rad-y}$ both $\approx 0.07$. The excitation of the radial-x band nearly vanishes, since $k_{729nm}$ is nearly at right angle to the x-vibration mode.
b) Sideband cooling for the axial and radial-y vibration. The ratio $P_{red}/P_{blue}$ yields a ground state probability of 90 % for the radial-y mode and better than 95% for the axial mode.

and $\nu_{radial}$. The observed linewidth for the transition on the carrier has been measured to be 1kHz ($\delta\nu/\nu = 2.5 \cdot 10^{-12}$) in the ac-power-line synchronized aquisition mode. The width of 1kHz is mostly caused by residual magnetic field fluctuations [11].

## 7 Ground state cooling of a single ion

For sideband cooling [18,17,12] the pulsed sideband spectroscopy pulse scheme is modified only slightly. The excitation of the $S_{1/2}-D_{5/2}$ transition is separated into two parts: During the first period, the cooling period, the transition $S_{1/2}-D_{5/2}$ is excited with full laser power (up to 130mW in 30$\mu$m waist) on the red sideband, at a laser detuning of $\Delta\nu = -\nu_{trap}$. The laser at 854nm is additionally switched on to broaden the $D_{5/2}$ level. The power of the 854nm radiation is adjusted for optimum cooling. In the second period, we probe the $S_{1/2}-D_{5/2}$ excitation probability $P_D(\nu)$. For the quantitative determination of the vibrational ground state probability $\langle p_{n=0}\rangle$ we compare $P_D(-\nu_{trap})$ and $P_D(\nu_{trap})$, i.e. on the red and sideband. If after cooling the vibrational ground state is reached with 100% probability, the excitation $P_D(-\nu_{trap})$ vanishes completely, as can be seen intuitively. If the phonon probability distribution $p_n$ is thermal, the ratio of excitation on the red and blue sideband is given by $P_{red}/P_{blue} = \langle n\rangle/(1+\langle n\rangle)$. In Fig. 4b we show results of sideband excitation after cooling, showing the ion to be in the ground state with more than 90% probability for the radial-y mode, and 95% probability in axial mode. The radial-x vibration was left uncooled. We succeded in simultaneous cooling of the radial-y *and* axial vibrational modes.

## 8 Driving coherent dynamics: Fock states

For coherent manipulation of the ion, such as e.g. the generation of nonclassical states [22], or entanglement [17], the lowest vibrational state in the ladder of phonon excitation is the ideal initial state. As a first example, namely the preparation of the vibrational Fock state $\mid n=1\rangle$, we first use a $\pi$ pulse at 729nm on the blue sideband $\mid n=0, S_{1/2}\rangle \rightarrow \mid n=1, D_{5/2}\rangle$, then we pump the ion with laser light at 854nm to $\mid n=1, S_{1/2}\rangle$. Since the oscillation frequency on the blue sideband scales like $\Omega_{n,n+1} = \Omega_0 \cdot \sqrt{n+1}$, we expect Rabi oscillations for the $\mid n=1\rangle$ Fock state to be $\sqrt{2}$ faster than starting with $\mid n=0\rangle$. We have excited Rabi oscillations on the axial blue sideband at $\delta\nu$ = 1.7MHz, see Fig. 5, and observed that the measured frequency ratio indeed agrees within 1% with the expected 1:$\sqrt{2}$ ratio.

## 9 Conclusion and outlook

Single trapped ions in a linear and in a three-dimensional Paul trap have been investigated. Individual state detection and state control, and the manipulation of vibration modes down to the fundamental ground state have been

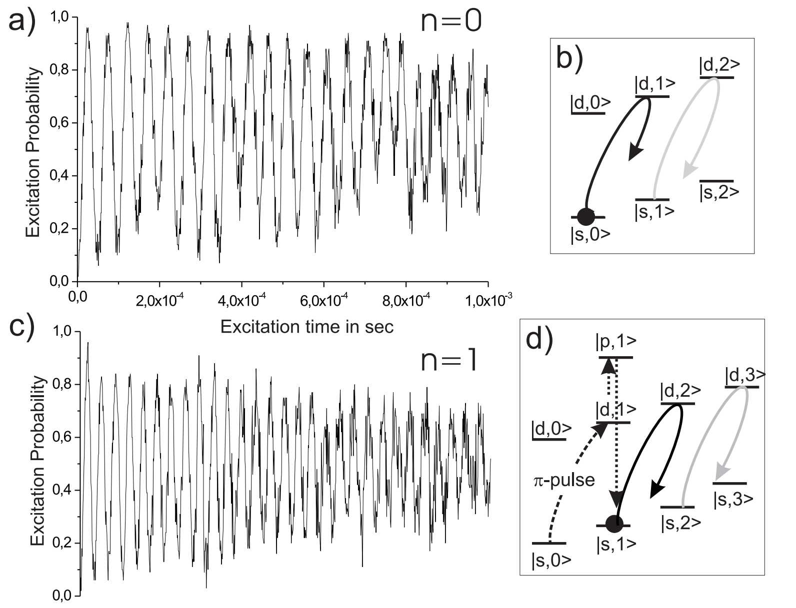


Figure 5. a) Rabi oscillations on the blue sideband starting in the ground state $\mid n = 0\rangle$. A large number of oscillations is observed and coherence is maintained for up to 1ms. Fourier analysis of the data indicates a probability of 89(1)% for n=0.
b) Principle of Rabi oscillation on the blue sideband.
c) Rabi oscillations as in (a) but now for the vibrational Fock state $\mid n = 1\rangle$. Note the higher oscillation frequency. Again, Fourier transformation yields a 88(1)% probability for n=1.
d) The method of state preparation for $\mid n = 1\rangle$ is indicated by the arrows:
$\mid n = 0, S_{1/2}\rangle \rightarrow \mid n = 1, D_{5/2}\rangle \rightarrow \mid n = 1, S_{1/2}\rangle$.

shown. In future experiments, we will extend our techniques to ensembles of two or more ions. For individual addressing of single ions in a string *and* their ground state cooling, an axial frequency of 0.5 - 0.7MHz as presently realized in our linear trap should be optimal,with inter-ion distances 7 - 9$\mu$m. Our first aims after cooling two ions to the vibrational ground state are the demonstration of a quantum gate between those ions, the generation and detection of Bell and GHZ states, and Ramsey spectroscopy using entangled states.

**Acknowledgments**

This work is supported by the Fonds zur Förderung der wissenschaftlichen Forschung within the Spezialforschungsbereich SFB15, and by the TMR networks "Quantum Information" (ERB-FMRX-CT96-0087), and "Quantum Structures" (ERB-FMRX-CT96-0077).

**References**

1. A. Ekert, in Atomic Physics **14**, 450, ed. D. J. Wineland, C. Wieman, S. J. Smith, AIP New York 1995. S. Haroche, et. al., in Atomic Physics **15**, 1. J. I. Cirac, et. al., in Atomic Physics **15**, 16. D. J. Wineland et. al., in Atomic Physics **15**, 31. ed. H. B. van den Heuvell, J. T. M. Walraven, M. W. Reynolds AIP New York 1996.
2. A. Ekert and R. Josza, Rev. Mod. Phys. **68** 3733, (1997).
3. J. I. Cirac, P. Zoller, Phys. Rev. Lett. **74**, 4091 (1995).
4. J. R. Anglin, J. P. Paz, and W. H. Zurek, Phys. Rev. A **55**, 4041 (1997).
5. C. A. Blockey, D. F. Walls, H. Risken, Europhys. Lett. **17**, 509 (1992).
6. J. I. Cirac, et. al., Phys. Rev. Lett. **70**, 762 (1993).
7. Proc. 5th Symp. Freq. Standards and Metrology, ed. J. C. Bergquist, (World Scientific, 1996).
8. D. J. Berkeland, et. al., Phys. Rev. Lett. **80**, 2089 (1998).
9. W. Paul, O. Osberghaus, and E. Fischer, Forschungsberichte des Wirtschafts- und Verkehrsministerium Nordrhein-Westfalen **415** (1958).
10. P. K. Ghosh, Ion traps, Clarendon, Oxford 1995.
11. H. C. Nägerl, et. al., Phys. Rev. A., submitted.
12. B. E. King, et. al., Phys. Rev. Lett. **81** 1525, (1998).
13. H. C. Nägerl, et. al., Appl. Phys. B **66**, 603 (1998).
14. D.J. Wineland, et. al., Journal of Research of the National Institute of Standards and Technology **103**, 259 (1998).
15. D. J. Wineland, et. al., Phys. Rev. A **36** 2220, (1987).
16. H. C. Nägerl, D. Leibfried, G. Thalhammer, J. Eschner, F. Schmidt-Kaler, and R. Blatt, Phys. Rev. A **60** (1. July), in press.
17. C. Monroe, et. al., Phys. Rev. Lett. **74**, 4011 (1995).
18. F. Diedrich, et. al., Phys. Rev. Lett. **62**, 403 (1989).
19. Optics Express **3**, 89 (1998).
20. D. F. V. James, Appl. Phys. B **66**, 181 (1998).
21. C. Monroe, et. al., Phys. Rev. Lett. **75**, 4714 (1995).
22. D. Leibfried, et. al., Phys. Rev. Lett **77**, 4281 (1996).